

MEASUREMENT OF NEUTRON-INDUCED NEUTRON-PRODUCING CROSS SECTIONS
OF ${}^6\text{Li}$ AND ${}^7\text{Li}$ AT 18.0 MeV

Satoshi CHIBA

Department of Physics, Japan Atomic Energy Research Institute
Tokai-mura, Ibaraki-ken 319-11, JapanMamoru BABA, Naohiro YABUTA, Tsukasa KIKUCHI, Masumi ISHIKAWA,
Naohiro HIRAKAWA and Kazusuke SUGIYAMAFaculty of Nuclear Engineering, Tohoku University
Sendai-shi, Miyagi-ken 980, Japan

Abstract: The energy and angular double-differential neutron emission cross sections (DDX), $d^2\sigma/dE'd\Omega$, of ${}^6\text{Li}$ and ${}^7\text{Li}$ have been measured at 12 angles from 30 to 150° with incident neutrons of 18.0 MeV. The measurement was based on the time-of-flight (TOF) method. Measured DDXs have been compared with predictions from evaluated nuclear data and some problems with the evaluations were found. It was also found that the angular distributions of the continuum energy neutrons have a clear systematic trend that is dependent on their Q-values. Neutrons corresponding to low excitation energy in residual nucleus showed strong forward angular distributions. A spherical optical model calculation was performed for the elastically scattered neutrons of ${}^6\text{Li}$. The continuum neutron spectra of ${}^6\text{Li}$ were analyzed in terms of the Final-State Interaction theory. The analysis could reproduce the experimental spectra very well with a large contribution from the ${}^3\text{S}_1$ partial wave in the d- α system.

(Measured DDX, ${}^6\text{Li}$, ${}^7\text{Li}$, 18.0 MeV, time-of-flight, evaluated nuclear data, optical model calculation, angular distribution, Final-State Interaction)

Introduction

In the past several years, neutron nuclear data have been investigated intensively below 14 MeV both from an experimental and a calculational point of view, mainly aiming at applications in the D-T fusion reactors. The status of the data base is, however, extremely poor above 14 MeV. Lately, the nuclear data in the higher energy range have become more and more important, relevant to radiation shielding for high energy accelerators, and such biomedical applications as cancer therapy with energetic particle beams.

The neutron nuclear data of ${}^6\text{Li}$ and ${}^7\text{Li}$ are of special importance, because they are the major tritium breeding materials in fusion applications. When neutrons are incident on lithium isotopes, several few-body break-up reactions take place, e.g., ${}^6\text{Li}(n,n'd)\alpha$, ${}^7\text{Li}(n,n't)\alpha$ and ${}^7\text{Li}(n,2nd)\alpha$ reactions. The mechanisms of these reactions are complicated and hence not understood well at present. Furthermore, even the systematics of the basic parameters of the optical model potential is not well established yet. Therefore, the significance of experimental data on the neutron cross sections of lithium isotopes is very high for both basic and applied research fields.

The aim of the present work is to measure the energy-angle double differential neutron-induced neutron-producing cross sections of ${}^6\text{Li}$ and ${}^7\text{Li}$ at an incident neutron energy of 18.0 MeV to give a data base for above requirements. They will be also used for future improvements of the JENDL library.

Experimental Procedure and Data Reduction

The experiment was performed using the neutron TOF spectrometer installed in the Fast Neutron Laboratory, Tohoku University/1/. The source neutrons were produced by the T(d,n) α

reaction. The deuteron beam was chopped and bunched to 3-ns width in the high energy terminal of the 4.5-MV Dynamitron accelerator and accelerated up to 2.2 MeV. About 1 μA of d^+ was incident on a Ti-T (8Ci of T) target at a repetition rate of 2MHz.

The scattering samples were enriched metallic lithium (94.5% in ${}^6\text{Li}$ and 99.9% in ${}^7\text{Li}$). They are cylindrical in shape; 3.2cm in diameter and 4.0cm in height. A polyethylene and a graphite sample were also used to determine the detector efficiency. Relative detection efficiency was also determined by measuring the energy spectrum of prompt neutrons emitted from the spontaneous fission of ${}^{252}\text{Cf}$.

The scattering samples were located 12cm from the neutron source at 0-deg. with respect to the deuteron beam. Neutrons scattered from these samples were detected by a 12.5-cm diameter by 5-cm thick NE213 liquid scintillation detector that was placed about 5 to 6 m from the scatterer. This detector was shielded by a large water tank. A 60-cm long copper shadow bar, an iron pre-collimator and a paraffine main collimator were set between the neutron source and the detector. The TOF spectra were measured at 12 angles between 30 and 150°. A 5-cm diameter by 5-cm thick NE213 scintillator was used to normalize the relative neutron flux. For both detectors, pulse shape discrimination circuits were used and γ -ray backgrounds were successfully rejected. Two bias settings were used for the main detector/2/; one with 0.3-MeV and another with 3-MeV proton equivalent.

The energy spectrum of the source neutrons is shown in Fig. 1. The energy of the main peak was measured to be 18.0 ± 0.4 MeV. The sub-peaks at about 5 and 2 MeV were formed by those neutrons produced from the D(d,n) and C(d,n) reactions, respectively. Contribution from the D(d,n) background neutrons caused no serious problems, because it produced a clear peak in the

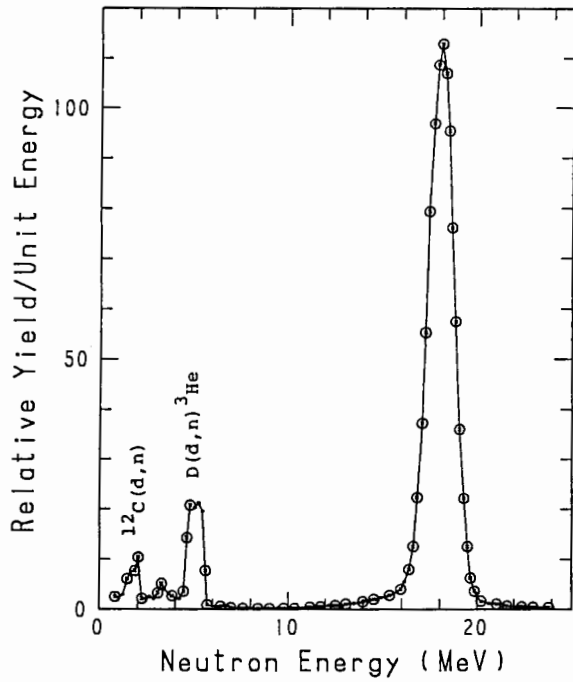


Fig.1 Source Neutron Energy Spectrum

TOF spectra of the scattered neutrons and hence could be subtracted easily. However, neutrons below the C(d,n) peak could not be assigned clearly. Therefore, the present paper will describe results obtained from 18.0 to 2.5-MeV range of the source neutron.

Measured TOF spectra were corrected for background and converted to energy spectra by the relativistic kinematics. Then effects of the finite sample size (source neutron anisotropy, multiple scattering and angular resolution) was corrected by the Monte-Carlo method^{2/}.

Results and Discussion

Comparison with the evaluated data

Examples of the measured DDXs are displayed in Figs. 2 and 3. The lines show predictions given in JENDL-3T/3/ for both nuclei, and ENDF/B-V for ⁶Li and ENDF/B-IV for ⁷Li. The evaluation curves were smeared considering the resolution of the experiment.

The JENDL-3T evaluation for ⁶Li predicts the overall shape of the DDX well. At forward angles, however, the experimental values below elastic peak are significantly larger than the evaluation. Especially the continuum neutron spectra above 8 MeV are enhanced considerably. Because in this region, the 2.19, 4.3 and 5.7 MeV levels in ⁶Li, i.e., the resonant states in the

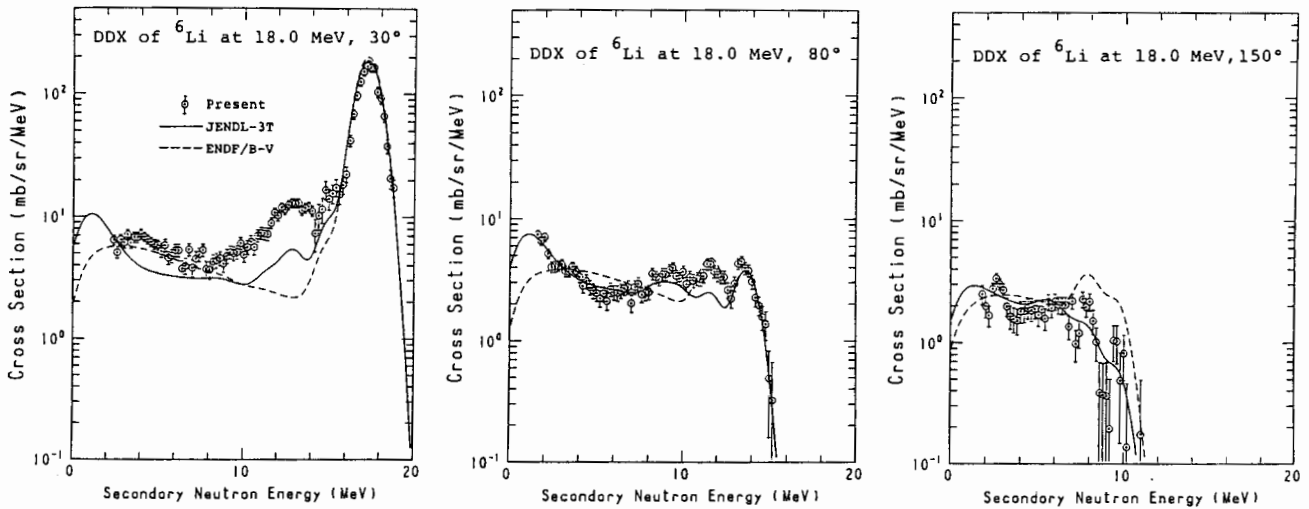


Fig.2 DDX of ⁶Li at 30, 80 and 150° measured with 18-MeV neutrons

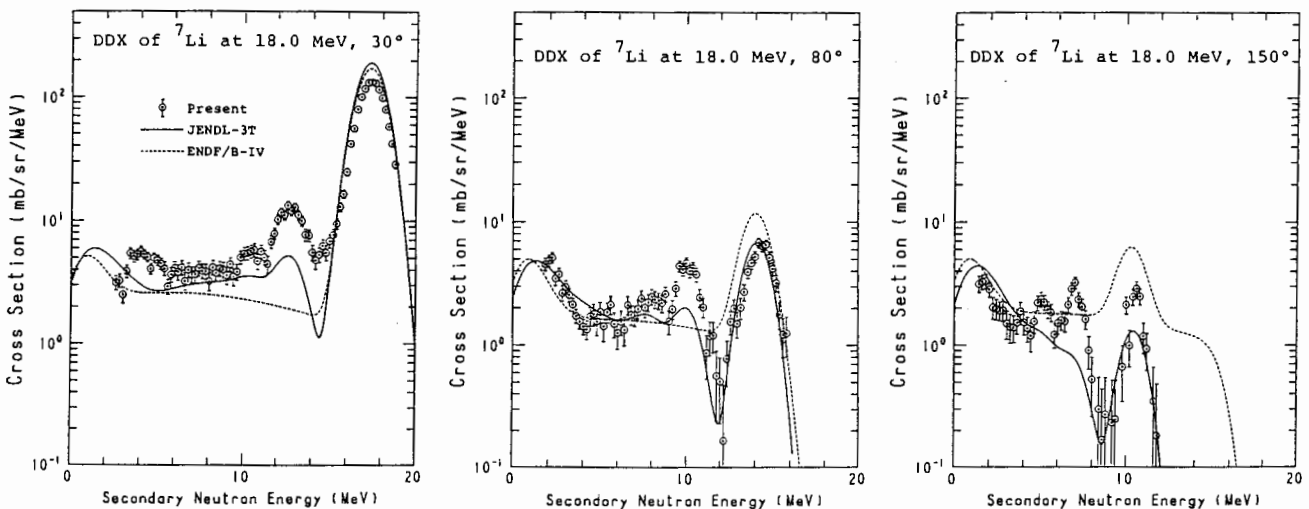


Fig.3 DDX of ⁷Li at 30, 80 and 150° measured with 18-MeV neutrons

d- α system, give the main contribution as shown later, the present results show that the final state interaction between d and α significantly affects the inelastic process.

As shown in Fig. 3, the JENDL-3T evaluation also underestimates the DDX of ${}^7\text{Li}$ at forward angles. It should be noted that the peak for the 4.63-MeV level is excited several times stronger than the JENDL-3T evaluation.

In Fig. 4 are shown the angular distributions of the ${}^6\text{Li}(n, n_0)$, ${}^7\text{Li}(n, n_0+n_1)$ and the ${}^7\text{Li}(n, n_2)$ reactions. The evaluated data reproduce the elastic scattering distributions well. However, the JENDL-3T evaluation for the 4.63-MeV state in ${}^7\text{Li}$ is underestimated at all angles.

Fig. 5 shows the angular distributions of continuum energy neutrons for several Q-value bins. It is clearly seen that there are clear systematic trends according to the Q-values for both nuclei: neutrons corresponding to small values of $|Q|$ exhibit strong forward distributions, while those to larger $|Q|$ values being almost isotropic. Furthermore, where Q-value bins are equal, the distributions are almost identical between ${}^6\text{Li}$ and ${}^7\text{Li}$. This result resembles one found by Kalbach et al./4/ in medium-weight mass range for pre-equilibrium (or multistep direct) and equilibrium neutron emission. In case of lithium, however, it is not plausible that the strong forward shape is caused by the pre-equilibrium process. Therefore, it

should be concluded that a considerable portion of the neutrons in the low excitation region was emitted through the direct reaction process. At present, however, it is not clear whether this similarity of the angular distributions of continuum neutrons for ${}^6\text{Li}$ and ${}^7\text{Li}$ is also true or not at other energies and other light elements.

Optical Model Calculation for ${}^6\text{Li}$

In this section, the spherical optical model (SOM) calculation was applied for ${}^6\text{Li}$. The calculation was made by code ECIS79/5/ and the best fit optical model parameters (OMP) were searched. Several sets of initial potentials were employed. Among them, those of Watson et al/6/ gave the best result. In the calculation, however, the spin-orbit term was fixed to the Thomas-Fermi type form factor, instead of a modified type used in Ref. 6.

Present deduced best fit parameters are as follows:

$$\begin{aligned} V &= 61.5 \text{ MeV}, r = 1.13, a = 0.62 \text{ fm} \\ W &= 10.5 \text{ MeV}, r_1 = 1.31, a_1 = 0.50 \text{ fm} \\ V_{\text{so}}^S &= 5.5 \text{ MeV}, r_{\text{so}} = 1.15, a_{\text{so}} = 0.50 \text{ fm (fixed)}. \end{aligned}$$

The solid line in Fig.6 shows the results calculated with these parameters. Agreement with the experimental data is excellent. The volume integral/nucleon of the present deduced real potential gives $705.5(\text{MeV}\cdot\text{fm}^3)$. This value lies in the middle between Watson et al's (587.7) and Dave et al's/7/ (885.6) potential.

Final-State Interaction Calculation of the Continuum Neutron Spectra for ${}^6\text{Li}$

As an analysis of the continuum energy neutron spectra for ${}^6\text{Li}$, a final-state interaction (FSI) theory was applied.

In the present analysis, the reaction ${}^6\text{Li}(n, n')$ was assumed to proceed via the following three major steps:

- 1) $n' + d + \alpha$: simultaneous break-up
- 2) $n' + {}^6\text{Li}^*$, ${}^6\text{Li}^* \rightarrow d + \alpha$: through final-state interaction between d and α
- 3) $d + {}^5\text{He}$, ${}^5\text{He} \rightarrow n' + \alpha$: two-step reaction via the ground state of ${}^5\text{He}$.

Assuming that these processes occur

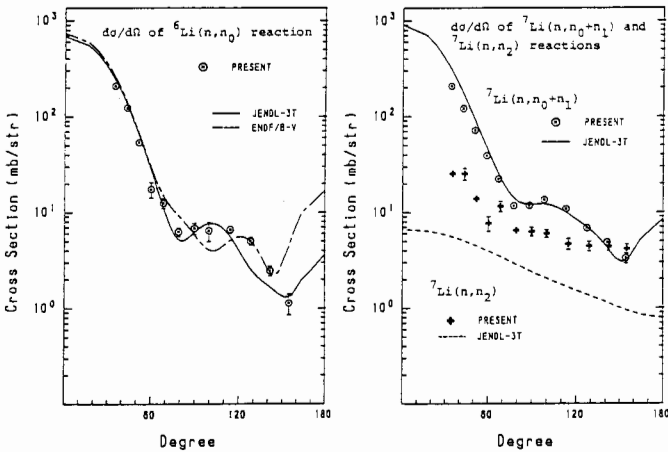


Fig.4 $d\sigma/d\Omega$ of ${}^6\text{Li}(n, n_0)$, ${}^7\text{Li}(n, n_0+n_1)$ and ${}^7\text{Li}(n, n_2)$ ${}^7\text{Li}(4.63)$ reactions

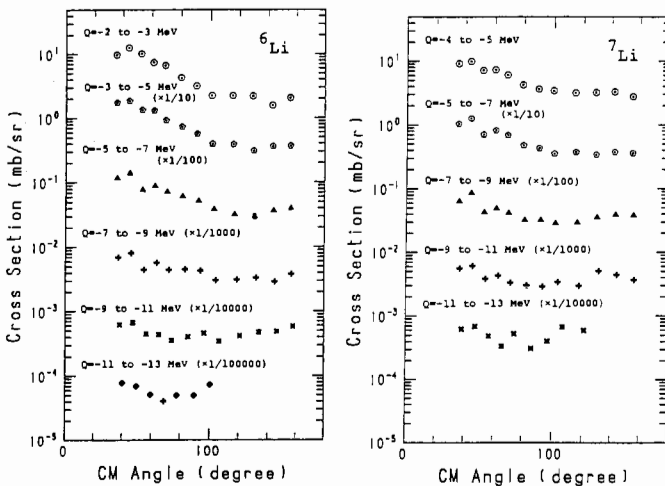


Fig.5 Angular distributions of the continuum energy neutrons in CM

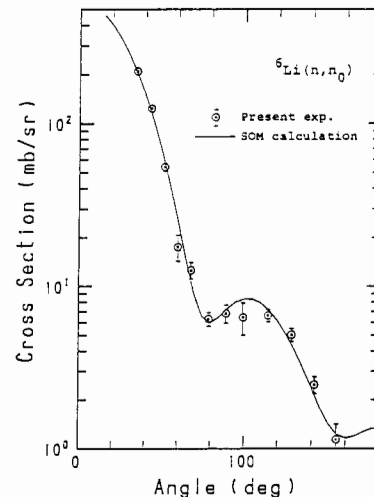


Fig.6 Angular distribution of the elastically scattered neutrons from ${}^6\text{Li}$

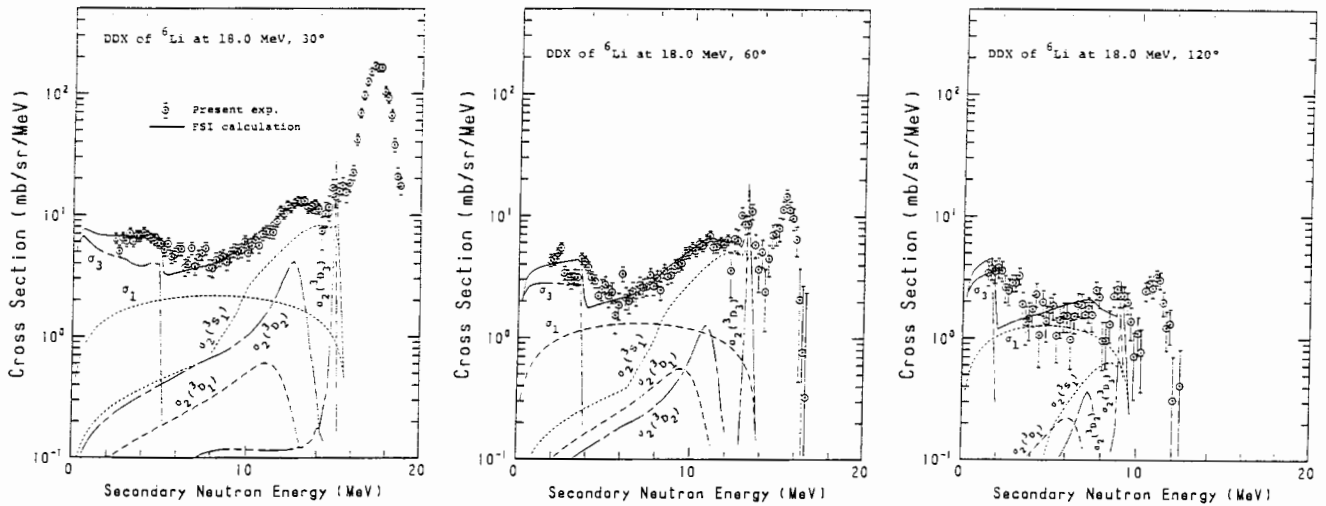


Fig.7 Comparison of the FSI calculation with the experimental data

incoherently, the continuum neutron producing cross section can be written as follows:

$$\sigma(n, n') = C_1\sigma_1 + C_2\sigma_2 + C_3\sigma_3 \quad (1)$$

where σ_i denotes the cross section corresponding to process i described above, and C_i the normalization factor which should be determined empirically. The σ_1 was taken to be the three body phase space distribution/8/, and σ_3 was set equal to the sequential decay reaction cross section that was formulated by Beynon and Oastler/9/. The σ_2 was calculated according to the following equation.

$$\sigma_2 = \sum_{LJ} C_{LJ} \cdot \sin^2(\delta_{LJ}) \frac{F_L^2(ka) + G_L^2(ka)}{(ka)^2} \cdot \rho \quad (2)$$

where

J:total spin in the $d+\alpha$ system in final state,

L:orbital angular momentum in the $d+\alpha$ system,

δ_{LJ} :phase shift of the $d+\alpha$ scattering in partial wave L_J ,

F_L, G_L :Coulomb wave functions of order L which are regular and irregular at the origin, respectively,

k :wave number of the relative motion of d and α ,

a :channel radius and was taken to be 4 fm,

ρ :three-body phase-space volume,

C_{LJ} :normalization factor for each partial wave.

This expression is from Ref.10. For the partial wave states of $d + \alpha$ system, four combinations of L_J were taken: 3S_1 , 3D_1 , 3D_2 and 3D_3 .

The calculated results are shown by the solid lines in Fig. 7. The contribution from each component is also plotted by the dashed or dash-dotted curve. Agreement between the measured and calculated cross sections is generally very good. Among the four partial waves in process 2, the 3S_1 wave gives the maximum contribution in the high energy range of the continuum spectra. This observation is in contradiction with what was found in heavy ion physics. Sakuragi et al. showed that, in $^{28}\text{Si}(^6\text{Li}, ^6\text{Li})^{28}\text{Li}$ reaction at 99 MeV, S-wave break-up of the projectile contributes less than 30% of D-wave break-up from their coupled-channel calculation with a microscopic form factor/11/. This fact reveals that the effective nucleon-nucleon force and reaction mechanism are differ-

ent between nucleon induced and heavy ion induced break-up of lithium nuclei. It should be noted, however, the present calculation is not final, because the resolution of the experiment and $(n, 2n)$ process are neglected.

Conclusion

The neutron-induced neutron-producing cross sections of ^6Li and ^7Li have been measured at 18.0 MeV by the time-of-flight method. The measured results were compared with the predictions in evaluated nuclear data libraries and several problems with the evaluations were found. The angular distribution of the continuum inelastic neutrons showed a clear systematic trend. Distributions for the low values of $|Q|$ revealed a strong forward shape: an evidence of the existence of the direct reaction mechanism.

The elastic scattering angular distribution of ^6Li was successfully analyzed by SOM.

The continuum neutron spectra emitted from $^6\text{Li}(n, n')$ reaction were calculated by the final-state interaction theory and compared with experiment. It was found that the FSI between d and α in the 3S_1 partial wave state gives a large contribution in the high energy part of the continuum neutron spectra. Further analysis will be continued for both of ^6Li and ^7Li as a future work.

REFERENCES

- 1.M.Baba et al.:JAERI-M 86-080, 270(1986).
- 2.S.Chiba et al.:Jour. Nucl. Sci. Technol., 22, 771(1985).
- 3.JENDL Compilation group:"JENDL-3T", a temporarily version of JENDL-3 of which a part will be revised.
- 4.C.Kalbach and F.M.Mann:Phys. Rev. C11, 112(1981).
- 5.J.Raynal:NOTES on ECIS79, unpublished.
- 6.B.A.Watson et al.:Phys. Rev., 182, 977(1969).
- 7.J.H.Dave and C.R.Gould:Phys. Rev., C28, 2212(1983).
- 8.G.G.Ohlsen:Nucl.Instr.Methods, 37, 240(1965).
- 9.T.D.Beynon and A.J.Oastler:Ann. Nucl. Energy, 6, 527(1979).
- 10.T.Rausch et al.:Nucl. Phys., A222, 429(1974).
- 11.Y.Sakuragi et al.:Prog.Theor. Phys., 70, 1047(1983)